Published in final edited form as:
J Mol Med (Berl). 2010 July ; 88(7): 665–675. doi:10.1007/s00109-010-0613-6.

Heme oxygenase-1 gene delivery by *Sleeping Beauty* inhibits vascular stasis in a murine model of sickle cell disease

John D. Belcher,
Division of Hematology, Oncology and Transplantation, Department of Medicine, University of Minnesota, 420 Delaware St SE, MMC 480, Minneapolis, MN 55455, USA; Vascular Biology Center, University of Minnesota, Minneapolis, MN 55455, USA

Julie V. Vineyard,
Division of Hematology, Oncology and Transplantation, Department of Medicine, University of Minnesota, 420 Delaware St SE, MMC 480, Minneapolis, MN 55455, USA; Vascular Biology Center, University of Minnesota, Minneapolis, MN 55455, USA

Carol M. Bruzzone,
Division of Hematology, Oncology and Transplantation, Department of Medicine, University of Minnesota, 420 Delaware St SE, MMC 480, Minneapolis, MN 55455, USA; Vascular Biology Center, University of Minnesota, Minneapolis, MN 55455, USA; Division of Gastroenterology, Department of Medicine, and Department of Genetics, Cell Biology and Development, University of Minnesota, 420 Delaware St SE, MMC 36, Minneapolis, MN 55455, USA

Chunsheng Chen,
Division of Hematology, Oncology and Transplantation, Department of Medicine, University of Minnesota, 420 Delaware St SE, MMC 480, Minneapolis, MN 55455, USA; Vascular Biology Center, University of Minnesota, Minneapolis, MN 55455, USA

Joan D. Beckman,
Division of Hematology, Oncology and Transplantation, Department of Medicine, University of Minnesota, 420 Delaware St SE, MMC 480, Minneapolis, MN 55455, USA; Vascular Biology Center, University of Minnesota, Minneapolis, MN 55455, USA

Julia Nguyen,
Division of Hematology, Oncology and Transplantation, Department of Medicine, University of Minnesota, 420 Delaware St SE, MMC 480, Minneapolis, MN 55455, USA; Vascular Biology Center, University of Minnesota, Minneapolis, MN 55455, USA

Clifford J. Steer, and
Division of Gastroenterology, Department of Medicine, and Department of Genetics, Cell Biology and Development, University of Minnesota, 420 Delaware St SE, MMC 36, Minneapolis, MN 55455, USA

Gregory M. Vercellotti

Correspondence to: Gregory M. Vercellotti, verce001@umn.edu.

Authorship contributions John D. Belcher designed the research, analyzed data, and wrote the paper. Julie V. Vineyard performed the research and analyzed the data. Carol M. Bruzzone performed the research, analyzed the data, and wrote the paper. Chunsheng Chen performed the research and analyzed the data. Joan D. Beckman performed research, analyzed data, and wrote the paper. Julia Nguyen performed the research and analyzed the data. Clifford J. Steer designed the research, analyzed the data, and wrote the paper. Gregory M. Vercellotti designed the research, analyzed data, and wrote the paper.

Disclosure of conflicts of interest The authors of this paper have no conflicts of interest to disclose

Division of Hematology, Oncology and Transplantation, Department of Medicine, University of Minnesota, 420 Delaware St SE, MMC 480, Minneapolis, MN 55455, USA; Vascular Biology Center, University of Minnesota, Minneapolis, MN 55455, USA

Gregory M. Vercellotti: verce001@umn.edu

Abstract

Increases in heme oxygenase-1 (HO-1) and administration of heme degradation products CO and biliverdin inhibit vascular inflammation and vasoocclusion in mouse models of sickle cell disease (SCD). In this study, an albumin (alb) promoter-driven *Sleeping Beauty* (*SB*) transposase plasmid with a wild-type rat *hmox-1* (wt-HO-1) transposable element was delivered by hydrodynamic tail vein injections to SCD mice. Eight weeks after injection, SCD mice had three- to five-fold increases in HO-1 activity and protein expression in liver, similar to hemin-treated mice. Immunohistochemistry demonstrated increased perinuclear HO-1 staining in hepatocytes. Messenger RNA transcription of the *hmox-1* transgene in liver was confirmed by quantitative real-time polymerase chain reaction restriction fragment length polymorphism (qRT-PCR RFLP) with no detectible transgene expression in other organs. The livers of all HO-1 overexpressing mice had activation of nuclear phospho-p38 mitogen-activated protein kinase (MAPK) and phospho-Akt, decreased nuclear expression of nuclear factor-kappa B (NF-κB) p65, and decreased soluble vascular cell adhesion molecule-1 (sVCAM-1) in serum. Hypoxia-induced stasis, a characteristic of SCD, but not normal mice, was inhibited in dorsal skin fold chambers in wt-HO-1 SCD mice despite the absence of *hmox-1* transgene expression in the skin suggesting distal effects of HO activity on the vasculature. No protective effects were seen in SCD mice injected with nonsense (ns-) rat *hmox-1* that encodes carboxy-truncated HO-1 with little or no enzyme activity. We speculate that HO-1 gene delivery to the liver is beneficial in SCD mice by degrading pro-oxidative heme, releasing anti-inflammatory heme degradation products CO and biliverdin/bilirubin into circulation, activating cytoprotective pathways and inhibiting vascular stasis at sites distal to transgene expression.

Keywords

Gene therapy; Heme oxygenase; Sickle cell disease; *Sleeping Beauty*

Introduction

Sickle cell disease (SCD) is an unrelenting hemolytic disease caused by a single base pair mutation in the β-globin chain of hemoglobin (Hb). SCD is characterized by recurring episodes of painful vasoocclusion, leading to ischemia–reperfusion injury and organ damage. Polymerization of hemoglobin-S (HbS) in the deoxy conformation shortens the lifespan of sickle erythrocytes and promotes intravascular hemolysis. When erythrocytes are lysed, extracellular hemoglobin is released and easily oxidized from ferrous (Fe^{2+}) to ferric (Fe^{3+}) hemoglobin (methemoglobin), which in turn, readily releases heme into the vasculature [1].

Heme is a potent inducer of vascular inflammation [2]. In SCD mice, the combination of heme-induced oxidative stress, inflammation, and the adhesion of circulating blood cells to vascular endothelium is a key driver of the proinflammatory and prothrombogenic vasculature that promotes sludging and stasis of blood flow in the postcapillary venules [3,4]. Cells defend or adapt to heme-mediated oxidative stress by inducing HO-1 to degrade heme. In animal models, increased expression of HO-1 has been shown to protect tissues and cells against ischemia–reperfusion injury, oxidative stress, inflammation, transplant rejection, apoptosis, and cell proliferation [5,6]. Conversely, HO-1 gene null mice

(*hmox-1*$^{-/-}$) and human patients deficient in HO-1 are especially prone to oxidative stress and inflammation [2,7,8]. The central importance of this protective system was recently highlighted by a child diagnosed with HO-1 deficiency, who exhibited extensive endothelial damage [8].

Not surprisingly, SCD patients and mice have elevated HO-1 in response to chronic hemolysis [2,9,10]. HO-1 expression is increased four- to sixfold in the organs of sickle mice compared to normal C57BL6 mice [2,9,10]. However, the level of HO-1 expression in SCD patients and mice may be inadequate. Vascular defenses against heme, including HO-1, can be overwhelmed during a hemolytic crisis resulting in heme-induced oxidative stress, inflammation, and vasoocclusion. Transgenic sickle mice expressing β^S hemoglobin have activated vascular endothelium that exhibits enhanced expression of NF-κB and adhesion molecules that promote vascular stasis in sickle, but not normal mice in response to hypoxia [3,10,11]. However, further induction of HO-1 in sickle mice with daily hemin injections for 3 days or administration of HO-1-adenovirus inhibits NF-κB activation, adhesion molecule expression, leukocyte–endothelium interactions, and hypoxia-induced vascular stasis [10]. Remarkably, administration of HO-1 products, CO or biliverdin to SCD mice, mimics the effects of HO-1 overexpression. Conversely, inhibition of HO-1 activity by tin protoporphyrin exacerbates hypoxia-induced stasis in sickle mice. Thus, HO enzyme activity plays a vital role in the inhibition of vasoocclusion in sickle mice.

In this study, we treated the S+S-Antilles sickle mouse model with *hmox-1* gene therapy targeted to the liver and evaluated the effects on cytoprotective pathways and hypoxia-induced vasoocclusion in a dorsal skin fold chamber model. To transfer the rat HO-1 gene into mice, we cloned the rat *hmox-1* gene into a *cis Sleeping Beauty* transposase (*SB*-Tn) system with the transposase driven by an albumin promoter [12]. The *SB*-Tn system was developed by resurrecting nonfunctional remnants of an ancient vertebrate transposable element from salmonid fish [13]. *SB*-Tn has features that make it particularly attractive as a vector for gene therapy. It can accommodate a much larger transgene than viral vectors, it is nonviral, it does not induce an immune inflammatory response in rodent models, and it mediates efficient stable transgene integration that exhibits persistent expression. Here, we report that *SB*-Tn-mediated HO-1 gene delivery to the livers of S+S-Antilles sickle mice leads to sustained (8 weeks+) HO-1 transgene expression, an increase in HO enzyme activity and cytoprotective signaling pathways in the liver, and distal inhibition of hypoxia-induced vascular stasis in the skin.

Methods

Mice

All animal experiments were approved by the University of Minnesota's Institutional Animal Care and Use Committee. We utilized male and female S+S-Antilles [14] transgenic sickle mice as a model for human SCD. The S+S-Antilles mice are on a C57BL/6 genetic background, are homozygous for deletion of the mouse β^{major} globin locus, and express human α, β^S, and $\beta^{S\text{-}Antilles}$ globin transgenes. $\beta^{S\text{-}Antilles}$ globins contain, in addition to the β^S mutation at β6, a second mutation at β23 (Val→Ile). $\beta^{S\text{-}Antilles}$ has low oxygen affinity and decreased solubility under deoxygenated conditions, resulting in a more severe form of SCD. In the S+S-Antilles mice, approximately 42% of the β globins expressed are β^S, and 36% are $\beta^{S\text{-}Antilles}$. These animals have moderately severe organ pathology [15].

The mice used in these studies were 17–23 weeks of age at sacrifice. The mice weighed 25–35 g and were housed in specific pathogen-free housing to prevent common murine infections that could cause an inflammatory response. All the mice were maintained on a standard chow diet.

Rat HO-1 plasmids

For in vivo experiments in mice, a rat *hmox-1* pBluescript plasmid containing an SV40 enhancer, a Friend's Spleen Focus-Forming Virus LTR promoter, the entire coding region of the wild-type (wt) rat *hmox-1* gene, and SV40 polyadenylation [16] was blunt cloned between two direct repeat (DR) binding sites within two inverted repeat (IR) sites (IR/DR) into a 2-kb, albumin (Alb)-driven, *SB*10 transposase plasmid [12]. The IR/DR elements act as essential binding sites for the transposase [17]. To prepare this construct, the *hmox-1* plasmid was digested with *HindIII* and *SalI*, and the resulting enhancer, promoter, coding region, and polyadenylation segment (1,600 bp) were separated from the vector backbone by agarose gel electrophoresis and purified using a Qiagen gel purification kit. The purified *hmox-1* construct was treated with Klenow to generate blunt ends. A second construct containing an Alb-driven *SB*10 transposase (4,193 bp), inserted outside a pair of IR/DRs (Alb/*SB*10/IRDR), was prepared from a pCMV *SB*10 plasmid using *EcoRI* and *XhoI* [13] and purified using a Qiagen™ plasmid isolation kit. The purified Alb/*SB*10/IRDR plasmid was opened at a unique *EcoRI* site between the IR/DRs and phosphatase treated. The prepared *SB*10 vector and *hmox-1* constructs were ligated overnight at 16°C with the *hmox-1* DNA inserted between the IR/DRs of the *SB*10 vector. Clones were screened by restriction digest mapping and sequencing followed by protein expression in tissue culture, HO-1 western blot analysis, and HO enzyme activity. The resultant clone (*SB*-wt-HO-1, 5,793 bp) expressed wt rat HO-1 (wt-HO-1) as previously described [12].

A nonsense rat *hmox-1* (ns-HO-1) control vector was constructed by inserting 4 bp containing an early stop codon into the *hmox-1* sequence of the *SB*-wt-HO-1 plasmid. To prepare this plasmid, *SB*-wt-HO-1 was digested at the unique type two restriction endonuclease site recognized by *NheI* (GCTAGC) occurring at bp723. The linearized plasmid was blunt filled with Klenow enzyme and religated with T4 ligase to create a four-nucleotide insertion shown in bold in the sequence below.

```
TTGAGGAGCTGCAGGCACTGCTGACAGAGGAACACAAAGACCAGAGTCCCTCACAGA
||||||||||||||||||||||||||||||||||||||||||||||||||||||||||
TTGAGGAGCTGCAGGCACTGCTGACAGAGGAACACAAAGACCAGAGTCCCTCACAGA

CAGAGTTTCTTCGCCAGAGGCCTG----CTAGCCTGGTTCAAGATACTACCTCTGCAG
|||||||||||||||||||||||||    ||||||||||||||||||||||||||||||
CAGAGTTTCTTCGCCAGAGGCCTGCTAGCTAGCCTGGTTCAAGATACTACCTCTGCAG

AGACGCCCCGAGGAAAAATCCCAGATCAGCACTAGTTCATCCCAGACACCGCTCCTGCGAT
||||||||||||||||||||||||||||||||||||||||||||||||||||||||||||
AGACGCCCCGAGGAAAAATCCCAGATCAGCACTAGTTCATCCCAGACACCGCTCCTGCGAT
```

Translation of that region in the wild-type clone includes amino acids (AA):

Ser Gln Thr Glu Phe Leu Arg Gln Arg Pro Ala Ser Leu Val Gln Asp Thr Thr Ser…

Translation is conserved for the Ser due to redundant coding but terminated by the 4-bp insertion immediately after the serine to create a ns codon:

Ser Gln Thr Glu Phe Leu Arg Gln Arg Pro Ala Ser C-term

The wt protein translates a 289-AA protein while the ns transcript translates a 241-AA carboxy-truncated protein. The *SB*-ns-HO-1 construct was screened as described above for *SB*-wt-HO-1. The resultant ns-HO-1 construct (*SB*-ns-HO-1, 5,797 bp) had no demonstrable enzymatic activity.

Gene transfer of rat hmox-1 into sickle mice

An *SB*-wt-HO-1 (*n*=4) or *SB*-ns-HO-1 (*n*=6) plasmid was delivered to S+S-Antilles sickle mice by hydrodynamic tail vein injection of 25 μg of plasmid DNA in 10% of the mouse's body weight (up to 2.5 ml) of sterile lactated Ringer's solution (LRS) [18]. Vehicle control

sickle mice (*n*=5) were injected with LRS without any DNA. Another group of control sickle mice were not injected with anything (*n*=7). Positive HO-1 control sickle mice (*n*=5) were injected intraperitoneally (ip) with hemin chloride (Calbiochem) at a dose of 40 μmol/kg/day) for 3 days. Eighteen hours after the third hemin injection, hypoxia-induced stasis was measured. Stock hemin chloride (10 mM) was prepared fresh daily by dissolving hemin chloride in 0.1 M NaOH in the dark. The stock hematin was diluted 1:10 (*v*/*v*) in LRS before ip injections into sickle mice.

Measurement of vascular stasis

Hypoxia-induced stasis of venular blood flow in the subcutaneous skin was measured in mice with an implanted dorsal skin fold chamber (DSFC) using intravital microscopy as previously described [3,19]. All measurements of blood flow parameters in the DSFC were made 3 days after DSFC implantation. Hypoxia-induced stasis of venular blood flow was measured 7–8 weeks after gene transfer. At baseline, with the mice in ambient air, flowing venules were selected at random and their relative locations were noted on a map of the microscopic field and recorded. After baseline selection of flowing venules in ambient air, the mice were subjected to 1 h of hypoxia (7% O_2/93% N_2), followed by reoxygenation in room air. After 1 h of reoxygenation, the same venules were re-examined for blood flow. Venules with no observable flow were counted as static. The percentage of static vessels was calculated by dividing the number of static venules by the total number of flowing venules selected at baseline. A minimum of 26 subcutaneous venules were examined in each mouse. We equated vascular stasis with vasoocclusion for experimental purposes. Certainly prolonged vasoocclusion seen clinically is associated with activation of coagulation and thrombosis leading to organ infarction.

Mouse tissue collection

After 4 h of reoxygenation, the mice in ambient air were sacrificed and tissues harvested as previously described [3]. Mice were asphyxiated in a CO_2 chamber for approximately 2 min. Blood was collected by cardiac puncture for isolation of serum. Organs were removed and divided for homogenate preparation, immunohistochemistry, and RNA isolation; wrapped in aluminum foil; frozen in liquid nitrogen; and later stored at −85°C. Liver sections from a subset of the mice were collected for immunohistochemistry and placed in 10% buffered formalin prior to embedding in paraffin blocks and sectioning. Dorsal skin was collected from mice for RNA isolation.

Homogenization of mouse livers and purification of liver nuclear extracts and microsomes

All liver processing and purifications were done on ice or at 4°C. The liver tissue, frozen in liquid nitrogen, was broken into small pieces with a hammer between layers of aluminum foil, then transferred to a mortar and reduced to a fine powder in liquid nitrogen. The thawed powder was homogenized on ice in 2 ml of buffer A containing 0.1% Triton X-100 (Sigma-Aldrich), 300 mM NaCl, 1.5 mM $MgCl_2$, 20 μM EDTA, 25 mM HEPES (*N*-2-hydroxyethylpiperazine-*N*′-2-ethanesulfonic acid) pH7.6 in a 5-ml Dounce tissue homogenizer (Wheaton) with 20 strokes of the tight-fitting pestle B. Cell debris was removed by centrifuging the crude homogenate at 500×*g* for 30 s at 4°C. Nuclei were pelleted by centrifuging aliquots of liver homogenates at 15,000×*g* for 5 min. Nuclear extracts were prepared by adding buffer B (Panomics, Nuclear Extraction Kit) to the nuclear pellet, sonicating for 10 s (Misonix) and incubating on ice for 2 h with gentle shaking. Samples were centrifuged at 15,000×*g* for 30 min, and nuclear extract supernatants were collected and stored at −85°C until use. Buffers A and B contained protease and phosphatase inhibitors at these final concentrations: 5 mM dithiothreitol, 0.1 mM orthovanadate, 20 mM β-glycerophosphate, 20 μg/ml leupeptin, 1 mM phenylmethane-sulfonylfluoride, and mammalian protease inhibitor cocktail (1:50, *v*/*v*; Sigma-Aldrich).

Liver microsomes were prepared by centrifuging the 15,000×*g* supernatants at 105,000×*g* for 1 h. Microsomal pellets were suspended in 2 mM $MgCl_2$, 0.1 M K_2HPO_4 buffer, pH7.4. Protein concentrations were measured in all samples using a Bio-Rad protein assay kit.

Measurement of HO enzyme activity in liver microsomes

HO activity was measured as previously described [20] in freshly isolated liver microsomes sonicated once for 10 s. Microsomes (2 mg) in 2 mM $MgCl_2$, 0.1 M K_2HPO_4 buffer, pH7.4, were added to the reaction mixture (400 μl, final) containing 2.5 μg of recombinant biliverdin reductase (Assay Designs), 2 mM glucose-6-phosphate, 0.2 U glucose-6-phosphate dehydrogenase, 50 μM hemin chloride, and 0.8 mM NADPH (Calbiochem) for 1 h in the dark. The bilirubin formed was extracted into chloroform, and the delta OD 464–530 nm was measured (extinction coefficient, 40 $mM^{-1}cm^{-1}$ for bilirubin). HO activity is expressed as picomole of bilirubin formed per milligram microsomal protein per hour.

Western blots of liver HO-1, p38 mitogen-activated protein kinase (MAPK), Akt, and NF-κB p65

An equal amount of liver microsomal (HO-1) or nuclear extract (p38, Akt, and p65) protein per lane was loaded in SDS buffer and subjected to electrophoresis on 10% or 15% polyacrylamide Tris–HCl gels (Bio-Rad). Afterward, the samples were transferred electrophoretically to polyvinylidene fluoride membranes (Millipore), and the membranes were probed with mouse monoclonal anti-HO-1 (Assay Designs), rabbit anti-phospho-p38 MAPK (residue Thr180/Tyr182), rabbit anti-phospho-Akt (residue Ser473; Cell Signaling Technology), or antinuclear factor-kappa B p65 (Santa Cruz Biotechnology). Sites of primary antibody binding were visualized with alkaline phosphatase-conjugated goat antimouse or goat antirabbit IgG (Santa Cruz Biotechnology). The final detection of immunoreactive bands was performed using an ECF™ substrate (GE Healthcare) and visualized on a Storm™ Reader (GE Healthcare). All membranes were stripped using Restore Stripping Buffer (Thermo Scientific) and reprobed with rabbit anti-GAPDH (Sigma-Aldrich), rabbit anti-p38 MAPK, or rabbit anti-Akt (Cell Signaling Technology). Bands were quantitated using Image J software (NIH).

RNA analysis

Total RNA was isolated from frozen organ sections, and HO-1 mRNA was quantitated by quantitative real-time polymerase chain reaction (qRT-PCR) as previously described [12]. The presence or absence of the wt- or ns-rat HO-1 transgene was confirmed by restriction fragment length polymorphism (RFLP) analysis of HO-1 cDNA using *ApaI* restriction enzyme digestion as previously described [12].

Immunohistochemistry

Formalin-fixed liver sections were processed routinely, embedded in paraffin, sectioned, and stained with mouse monoclonal anti-HO-1 (Assay Designs). Sites of primary antibody binding were visualized with horseradish peroxidase (HRP)-conjugated goat antimouse IgG (Biocare Medical). The final detection of HO-1 immunoconjugates was performed with the HRP substrates diaminobenzidine and H_2O_2. Nuclei were counterstained with hematoxylin.

Enzyme-linked immunosorbent assay for soluble vascular cell adhesion molecule-1 in serum

Serum levels of soluble vascular cell adhesion molecule-1 (sVCAM-1) were measured by enzyme-linked immunosorbent assay (ELISA) according to the manufacturer's protocol (R&D Systems, Minneapolis, MN).

Statistics

All statistical analyses were performed with SigmaStat 2.0 for Windows (SPSS Inc, Chicago, IL). Comparisons of multiple treatment groups (control, wt-HO-1, ns-HO-1, and hemin) to LRS-treated mice were made using one-way analysis of variance (ANOVA). The proportions of venules exhibiting stasis in each treatment group were compared using a *Z* test.

Results

S+S-Antilles sickle mice were injected hydrodynamically with an alb promoter-driven *cis* *SB*-Tn vector with either a wt rat *hmox-1* gene (wt-HO-1) or a ns-HO-1 containing an early stop codon. The two negative controls for this study included sickle mice that were not injected (control) and sickle mice hydrodynamically injected with LRS. Sickle mice injected three consecutive days with hemin served as positive controls.

Seven to 8 weeks after hydrodynamic *SB* injection or 18 h after the third hemin injection, the organs were removed and flash frozen. Microsomal membranes (n=2–4 mice per treatment group) were isolated from the livers, and 30 μg of microsomal protein from each liver was run on a western blot and immunostained for HO-1 protein expression (Fig. 1a). HO-1 protein bands at 32 kDa were quantified by densitometry (Fig. 1b). Mean HO-1 protein expression was increased in the livers of sickle mice injected with *SB*-wt-HO-1 (p<0.01), *SB*-ns-HO-1 (p< 0.05), or hemin (p<0.01) compared to mice injected with LRS vehicle. HO enzyme activity was increased in the livers of sickle mice injected with *SB*-wt-HO-1 (p<0.01) or hemin (p<0.05), but not in noninjected sickle mice (control) or in sickle mice injected with *SB*-ns-HO-1 (Fig. 1c).

Mean HO-1 to GAPDH mRNA ratios (Fig. 2a) were increased in the livers of sickle mice injected with either *SB*-wt-HO-1 (p<0.05), *SB*-ns-HO-1 (p<0.05), or hemin (p< 0.05). The presence or absence of wt- or ns-rat HO-1 mRNA in mouse tissue was confirmed by RFLP analysis of HO-1 cDNA. The rat *hmox-1* sequence has an *ApaI* restriction site which is absent in the mouse *hmox-1* sequence. After *ApaI* digestion, the mouse fragment is 212 bp, and the rat fragments are 92 and 120 bp. The rat fragments at 92 and 120 bp were present in the *ApaI* digests of cDNA produced from the mRNA isolated from the livers of sickle mice injected with *SB*-wt-HO-1 or *SB*-ns-HO-1, but not in control, LRS-, or hemin-treated mice (Fig. 2b). The mouse product at 212 bp was seen in all animals.

To determine the cellular location of HO-1 expression, formalin-fixed paraffin-embedded liver tissues from a subset of the mice were sectioned and stained with anti-HO-1 monoclonal antibody (Fig. 3). Immunostaining demonstrated HO-1 overexpression primarily in hepatocytes of animals treated with wt-HO-1, ns-HO-1, and hemin. HO-1 staining was primarily nonnuclear; this is consistent with the endoplasmic reticulum being the major site of HO-1 expression. However, some nuclear HO-1 staining was seen in hepatocytes of mice expressing ns-HO-1 (images not shown).

Western blots of liver nuclear extracts were immunostained for phospho- and total p38 MAPK and Akt expression (Fig. 4a, b). Activated phospho-p38 MAPK (Fig. 4a) and phospho-Akt (Fig. 4b) were elevated in liver nuclear extracts of sickle mice injected with *SB*-wt-HO-1 or hemin, but not in control, LRS-, or *SB*-ns-HO-1-treated mice. Total p38 MAPK (Fig. 4a) and Akt (Fig 4b) were not different between treatment groups. Thus, the p38 MAPK and Akt signal transduction pathways were activated only in mice with significantly increased HO enzyme activity.

Western blots of liver nuclear extracts also were immunostained for NF-κB p65 and quantified by densitometry (Fig. 4c). NF-κB p65 expression was lower in liver nuclear extracts of sickle mice injected with *SB*-wt-HO-1 ($p<0.05$) or hemin ($p<0.05$), but not in control or *SB*-ns-HO-1-treated mice compared to LRS mice. Hence, NF-κB p65 nuclear localization was decreased only in mice with significantly increased HO enzyme activity.

Serum levels of sVCAM-1 were measured by ELISA (Fig. 4d). sVCAM-1 was lower in serum from sickle mice injected with SB-wt-HO-1 ($p<0.05$) or hemin ($p<0.05$) compared to LRS mice; sVCAM levels were not significantly different in control and ns-HO-1-treated mice. Thus, sVCAM-1 levels in serum were lower only in mice with significantly increased HO activity.

Vascular stasis was measured in a DSFC model after hypoxia–reoxygenation using the S+S-Antilles mice as previously described [10,19]. After baseline selection of flowing venules, the mice were exposed to 1 h of hypoxia (7% O_2/93% N_2) followed by 1 h of reoxygenation in room air. After 1 h of reoxygenation, the same venules selected at baseline were re-examined for blood flow. The number of static venules exhibiting no blood flow were counted and expressed as a percentage of the total number of flowing venules selected at baseline (Fig. 5). Hypoxia-induced vascular stasis was inhibited in the skin of sickle mice injected with *SB*-wt-HO-1 ($p<0.05$) or hemin ($p<0.05$), but not in control, LRS-, or *SB*-ns-HO-1-treated mice. Thus, hypoxia-induced stasis in subcutaneous venules in the skin was inhibited only in sickle mice with significantly increased HO enzyme activity in their liver.

Since hypoxia-induced vascular stasis was inhibited in mice overexpressing enzymatically active HO-1, the dorsal skin of sickle mice was examined for the presence of rat *hmox-1* mRNA by qRT-PCR RFLP analysis. The rat *hmox-1 ApaI* fragments at 92 and 120 bp were absent in the dorsal skin samples (Fig. 6). Only the mouse product at 212 bp was seen in the skin of all mice. Rat hepatocytes were analyzed by qRT-PCR RFLP as controls and show the rat *hmox-1* fragments at 92 and 120 bp but not the mouse product at 212 bp (Fig 6). Moreover, qRT-PCR RFLP analysis found little or no detectible rat *hmox-1* transgene expression after 8 weeks in other mouse organs such as spleen which has the highest endogenous expression of HO-1 (data not shown).

Discussion

We have utilized an *SB* vector to deliver enzymatically active (wt, AA 1–289) and nonactive (ns, AA 1–241) forms of rat *hmox-1* to the livers of sickle mice. Expression of the rat *hmox-1* transgene in mouse livers was confirmed by enzyme activity, western blot, immunohistochemistry, and qRT-PCR RFLP analysis. Livers of sickle mice overexpressing wt-HO-1, but not ns-HO-1, had marked activation of the phospho-p38 MAPK and phospho-Akt cell signaling pathways, reduced levels of NF-κB p65 in liver nuclear extracts, and decreased sVCAM-1 in serum. Similarly, hypoxia-induced vascular stasis, a characteristic of sickle but not normal mice, was only inhibited in sickle mice overexpressing enzymatically active HO. Vascular stasis was inhibited in the venules of dorsal skin despite the absence of the rat *hmox-1* transgene in the skin suggesting that expression of the wt-*hmox-1* transgene in the liver had distal effects on the vasculature of sickle mice.

HO-1 has attracted much interest as a cytoprotective protein [21–27]. Most of the salutary effects of HO-1 overexpression can be reproduced by treating cells or animals with the byproducts of heme catabolism, CO, biliverdin, and iron-induced ferritin. In fact many, if not all, of the cytoprotective effects of HO-1 overexpression can be reproduced with low, nontoxic concentrations of CO [28–30], although biliverdin and heavy chain ferritin also have cytoprotective effects on cells and tissues [31,32]. HO-1 overexpression or treatment

with CO has antioxidative, anti-inflammatory, antiapoptotic, and antiproliferative effects and protects cells and tissues in numerous models of tissue injury and transplant rejection. These effects are dependent on the activation of the p38 MAPK and Akt signal transduction pathways [28,30]. In the liver, activation of the p38 MAPK and Akt pathways with HO-1 overexpression or CO treatment leads to marked resistance to apoptosis and hepatic injury induced by ischemia–reperfusion, TNF-α, LPS, carbon tetrachloride, CD95/Fas ligand, or transplantation [33–38]. We recently reported that phospho-p38 MAPK and phospho-Akt were markedly increased in the livers of SCD mice after treatment with intermittent inhaled CO at 250 ppm for 10 weeks [15]. In the current study, overexpression of HO-1 also induced phospho-p38 MAPK and phospho-Akt in the livers of SCD mice suggesting that heme degradation and CO production by HO-1 may have been responsible for induction of these cytoprotective pathways. This argument is strengthened by the observation that overexpression of enzymatically inactive HO-1 (ns-HO-1) did not activate these cytoprotective pathways. These systemic effects are consistent with HO-1 degrading excess heme, thereby reducing the oxidative and inflammatory tone of sickle mice and subsequent diffusion of CO and/or biliverdin/bilirubin out of the liver into circulation. It is important to note that our laboratory previously demonstrated that inhaled CO at 250 ppm or ip injection of biliverdin inhibits vascular stasis in the skin of sickle mice [10]. While levels of CO and bilirubin in the blood were not measured in these studies, future studies will address these potential mechanisms.

Vasoocclusion is a hallmark of SCD, and activation of vascular endothelium plays an essential role. Transgenic sickle mice, expressing human βS globins, have an activated vascular endothelium exhibited by increased NF-κB activation and adhesion molecule expression compared to normal mice [3,10,11]. Endothelial cell adhesion molecules play a critical role in vasoocclusion. VCAM-1, ICAM-1, or P-selectin blockade with monoclonal antibodies inhibits hypoxia-induced vasoocclusion and leukocyte adhesion and/or rolling in SCD mice [3,4]. Similarly, anti-inflammatory treatments such as dexamethasone, that inhibit endothelial cell activation and adhesion molecule expression, also inhibit vasoocclusion in SCD mice [3]. HO-1 overexpressing mice had decreased nuclear expression of NF-κB p65 in their livers and decreased sVCAM-1 in serum. It is believed that elevated levels of soluble endothelium-derived adhesion molecules in the plasma of SCD patients, and murine models of SCD occurs secondary to endothelial cell activation. Elevated levels of soluble endothelium-derived adhesion molecules in SCD patients are associated with pulmonary hypertension, organ dysfunction, and mortality [39]. Decreases in sVCAM-1 in serum are consistent with HO-1 overexpression having anti-inflammatory effects on vascular endothelium and inhibitory effects on vasoocclusion.

SCD patients and SCD mice typically have elevated white blood cell counts, which reflect the proinflammatory phenotype of SCD [3,10,11]. Treatment of SCD mice with 25 or 250 ppm inhaled CO for 1 h/day, 3 days/week for 8–10 weeks significantly decreases total mean white blood cell, neutrophil, and lymphocyte counts in peripheral blood [15]. In the current study, HO-1 gene therapy had no effect on the total mean white blood cell count; the mean white count was $15.8\times10^3/\mu l$ in both LRS- and wt-HO-1-treated SCD mice (data not shown). Thus, CO levels did not reach levels high enough to affect the white blood cell counts in HO-1 overexpressing SCD mice.

CO interactions with Hb can modulate hemolysis in SCD. CO binding to HbS shifts the oxygen dissociation curve to the left and inhibits HbS deoxygenation, HbS polymerization, and RBC hemolysis [40]. Since hepatic CO production may be increased in SCD mice overexpressing wt-HO-1, total serum heme levels were measured as a marker of hemolysis according to the method of Huy et al. [41]. Mean serum heme levels were 29 μM in LRS-treated mice and 19 μM in SCD mice overexpressing wt-HO-1, but these results were not

statistically different (data not shown). The S+S-Antilles mouse model used in these studies does not develop severe anemia warranting additional studies in a more hemolytic and anemic sickle mouse model.

In these studies, HO-1 was targeted to the liver using an *SB* transposase with an alb promoter. The transposase, delivered in *cis* with the *hmox-1* transgene, binds to IR/DR sites flanking the transgene, and catalyzes the excision of the flanked transgene, mediating its insertion into the target host genome with an apparently equal preference for AT-rich TA dinucleotide insertion sites in introns, exons, and intergenic sequences [42–45]. The alb promoter driving the transposase precludes significant insertion into nonhepatic chromosomes. This study did not look at insertion sites of the *hmox-1* transgene in livers as others have previously demonstrated that this *SB* vector readily integrates transgenes into mouse hepatocyte chromosomes [46]. Episomal expression of the transgene can occur in other organs earlier than 8 weeks, but decays until little or no episomal expression remains by 8 weeks.

Overexpression of HO-1 in nonhepatic tissues might also be beneficial in SCD. However, caution is warranted with HO-1 gene therapy when using ubiquitous, nontissue-specific promoters. It has been reported that continuous HO-1 transgene overexpression in HUVEC cells in culture results in downregulation of phospho-Akt expression [47]. This suggests that there could be tissue-specific effects of HO-1 gene therapy, and a targeted approach may be desirable.

Previous studies have reported cytoprotective effects of truncated and nonenzymatically active forms of HO-1 in cell culture [48,49]. HO-1 can lose 52 amino acids from its C terminus by proteolysis and travel from the endoplasmic reticulum to the nucleus where it can upregulate genes that promote cytoprotection against oxidative stress [48]. In images not shown, we saw some hepatocytes with nuclear HO-1 expression in sickle mice expressing ns-HO-1, which has 48 amino acids missing from the C terminus. However, no cytoprotective effects were seen in our study, suggesting that the beneficial effects of HO-1 gene therapy in sickle mice may be mediated primarily by heme degradation and production of CO and biliverdin by enzymatically active HO.

In conclusion, we used an *SB* vector containing an *hmox-1* gene that gives sustained overexpression of HO-1 in the livers of sickle mice. HO-1 overexpression in sickle mouse livers activates cytoprotective p38 MAPK and Akt signal transduction pathways, inhibits nuclear NF-κB p65 expression, reduces sVCAM-1 levels in serum, and inhibits hypoxia-induced vascular stasis distally in the skin. We speculate that *hmox-1* gene transfer could be beneficial in SCD by inhibiting oxidative stress, inflammation, vasoocclusion, and organ infarction. Future studies will examine the mechanisms and effects of *SB*-mediated *hmox-1* gene therapy on markers of oxidative stress, organ pathology, and lifespan in a more severe murine model of human SCD.

Acknowledgments

The rat *hmox-1* gene plasmid was a generous gift from Dr. Leo Otterbein and Dr. Jawed Alam. This work was supported by NHLBI grants R01 HL67367 and P01 HL55552. We would like to thank Drs. Robert Hebbel, Karl Nath, and Arne Slungaard for the constructive criticisms, Fuad Abdulla in Dr. Hebbel's laboratory for breeding and characterizing the S+S-Antilles sickle mice used for these studies, and Colleen Forster for her expert HO-1 immunohistochemistry.

References

1. Jay U. Methemoglobin—it's not just blue: a concise review. Am J Hematol. 2007; 82:134–144. [PubMed: 16986127]

2. Wagener FA, Eggert A, Boerman OC, Oyen WJ, Verhofstad A, Abraham NG, Adema G, van Kooyk Y, de Witte T, Figdor CG. Heme is a potent inducer of inflammation in mice and is counteracted by heme oxygenase. Blood. 2001; 98:1802–1811. [PubMed: 11535514]

3. Belcher JD, Mahaseth H, Welch TE, Vilback AE, Sonbol KM, Kalambur VS, Bowlin PR, Bischof JC, Hebbel RP, Vercellotti GM. Critical role of endothelial cell activation in hypoxia-induced vasoocclusion in transgenic sickle mice. Am J Physiol Heart Circ Physiol. 2005; 288:H2715–2725. [PubMed: 15665055]

4. Kaul DK, Hebbel RP. Hypoxia/reoxygenation causes inflammatory response in transgenic sickle mice but not in normal mice. J Clin Invest. 2000; 106:411–420. [PubMed: 10930444]

5. Otterbein LE, Soares MP, Yamashita K, Bach FH. Heme oxygenase-1: unleashing the protective properties of heme. Trends Immunol. 2003; 24:449–455. [PubMed: 12909459]

6. Wagener FADTG, Volk HD, Willis D, Abraham NG, Soares MP, Adema GJ, Figdor CG. Different faces of the heme-heme oxygenase system in inflammation. Pharmacological Reviews. 2003; 55:551–571. [PubMed: 12869663]

7. Yachie A, Niida Y, Wada T, Igarashi N, Kaneda H, Toma T, Ohta K, Kasahara Y, Koizumi S. Oxidative stress causes enhanced endothelial cell injury in human heme oxygenase-1 deficiency. J Clin Invest. 1999; 103:129–135. [PubMed: 9884342]

8. Kawashima A, Oda Y, Yachie A, Koizumi S, Nakanishi I. Heme oxygenase-1 deficiency: the first autopsy case. Hum Pathol. 2002; 33:125–130. [PubMed: 11823983]

9. Nath KA, Grande JP, Haggard JJ, Croatt AJ, Katusic ZS, Solovey A, Hebbel RP. Oxidative stress and induction of heme oxygenase-1 in the kidney in sickle cell disease. Am J Pathol. 2001; 158:893–903. [PubMed: 11238038]

10. Belcher JD, Mahaseth H, Welch TE, Otterbein LE, Hebbel RP, Vercellotti GM. Heme oxygenase-1 is a modulator of inflammation and vaso-occlusion in transgenic sickle mice. J Clin Invest. 2006; 116:808–816. [PubMed: 16485041]

11. Belcher JD, Bryant CJ, Nguyen J, Bowlin PR, Kielbik MC, Bischof JC, Hebbel RP, Vercellotti GM. Transgenic sickle mice have vascular inflammation. Blood. 2003; 101:3953–3959. [PubMed: 12543857]

12. Bruzzone CM, Belcher JD, Schuld NJ, Newman KA, Vineyard J, Nguyen J, Chen C, Beckman JD, Steer CJ, Vercellotti GM. Quantitative real-time polymerase chain reaction (qRT-PCR) restriction fragment length polymorphism (RFLP) method for monitoring highly conserved transgene expression during gene therapy. Transl Res. 2008; 152:290–297. [PubMed: 19059164]

13. Ivics Z, Hackett PB, Plasterk RH, Izsvak Z. Molecular reconstruction of Sleeping Beauty, a Tc1-like transposon from fish, and its transposition in human cells. Cell. 1997; 91:501–510. [PubMed: 9390559]

14. Fabry ME, Sengupta A, Suzuka SM, Costantini F, Rubin EM, Hofrichter J, Christoph G, Manci E, Culberson D, Factor SM, et al. A second generation transgenic mouse model expressing both hemoglobin S (HbS) and HbS-Antilles results in increased phenotypic severity. Blood. 1995; 86:2419–2428. [PubMed: 7662990]

15. Beckman JD, Belcher JD, Vineyard JV, Chen C, Nguyen J, Nwaneri MO, O'Sullivan MG, Gulbahce E, Hebbel RP, Vercellotti GM. Inhaled carbon monoxide reduces leukocytosis in a murine model of sickle cell disease. Am J Physiol Heart Circ Physiol. 2009; 297(4):H1243–H1253. [PubMed: 19617415]

16. Shibahara S, Muller R, Taguchi H, Yoshida T. Cloning and expression of cDNA for rat heme oxygenase. Proc Natl Acad Sci U S A. 1985; 82:7865–7869. [PubMed: 3865203]

17. Cui Z, Geurts AM, Liu G, Kaufman CD, Hackett PB. Structure-function analysis of the inverted terminal repeats of the sleeping beauty transposon. J Mol Biol. 2002; 318:1221–1235. [PubMed: 12083513]

18. Bell JB, Podetz-Pedersen KM, Aronovich EL, Belur LR, McIvor RS, Hackett PB. Preferential delivery of the Sleeping Beauty transposon system to livers of mice by hydrodynamic injection. Nat Protoc. 2007; 2:3153–3165. [PubMed: 18079715]

19. Kalambur VS, Mahaseth H, Bischof JC, Kielbik MC, Welch TE, Vilback A, Swanlund DJ, Hebbel RP, Belcher JD, Vercellotti GM. Microvascular blood flow and stasis in transgenic sickle mice:

utility of a dorsal skin fold chamber for intravital microscopy. Am J Hematol. 2004; 77:117–125. [PubMed: 15389823]

20. Balla G, Jacob HS, Balla J, Rosenberg M, Nath K, Apple F, Eaton JW, Vercellotti GM. Ferritin: a cytoprotective antioxidant strategem of endothelium. J Biol Chem. 1992; 267:18148–18153. [PubMed: 1517245]
21. Peterson SJ, Frishman WH. Targeting heme oxygenase: therapeutic implications for diseases of the cardiovascular system. Cardiol Rev. 2009; 17:99–111. [PubMed: 19384082]
22. Dulak J, Loboda A, Jozkowicz A. Effect of heme oxygenase-1 on vascular function and disease. Curr Opin Lipidol. 2008; 19:505–512. [PubMed: 18769232]
23. Abraham NG, Tsenovoy PL, McClung J, Drummond GS. Heme oxygenase: a target gene for anti-diabetic and obesity. Curr Pharm Des. 2008; 14:412–421. [PubMed: 18289068]
24. Soares MP, Bach FH. Heme oxygenase-1 in organ transplantation. Front Biosci. 2007; 12:4932–4945. [PubMed: 17569621]
25. Nath KA. Heme oxygenase-1: a provenance for cytoprotective pathways in the kidney and other tissues. Kidney Int. 2006; 70:432–443. [PubMed: 16775600]
26. Ryter SW, Alam J, Choi AM. Heme oxygenase-1/carbon monoxide: from basic science to therapeutic applications. Physiol Rev. 2006; 86:583–650. [PubMed: 16601269]
27. Maines MD. The heme oxygenase system: update 2005. Antioxid Redox Signal. 2005; 7:1761–1766. [PubMed: 16356137]
28. Kim HP, Ryter SW, Choi AM. CO as a cellular signaling molecule. Annu Rev Pharmacol Toxicol. 2006; 46:411–449. [PubMed: 16402911]
29. Piantadosi CA. Carbon monoxide, reactive oxygen signaling, and oxidative stress. Free Radic Biol Med. 2008; 45:562–569. [PubMed: 18549826]
30. Bilban M, Haschemi A, Wegiel B, Chin BY, Wagner O, Otterbein LE. Heme oxygenase and carbon monoxide initiate homeostatic signaling. J Mol Med. 2008; 86:267–279. [PubMed: 18034222]
31. Balla J, Vercellotti GM, Jeney V, Yachie A, Varga Z, Jacob HS, Eaton JW, Balla G. Heme, heme oxygenase, and ferritin: how the vascular endothelium survives (and dies) in an iron-rich environment. Antioxid Redox Signal. 2007; 9:1–19. [PubMed: 17115885]
32. Kapitulnik J, Maines MD. Pleiotropic functions of biliverdin reductase: cellular signaling and generation of cytoprotective and cytotoxic bilirubin. Trends Pharmacol Sci. 2009; 30:129–137. [PubMed: 19217170]
33. Amersi F, Shen XD, Anselmo D, Melinek J, Iyer S, Southard DJ, Katori M, Volk HD, Busuttil RW, Buelow R, Kupiec-Weglinski JW. Ex vivo exposure to carbon monoxide prevents hepatic ischemia/reperfusion injury through p38 MAP kinase pathway. Hepatology. 2002; 35:815–823. [PubMed: 11915027]
34. Kim HS, Loughran PA, Kim PK, Billiar TR, Zuckerbraun BS. Carbon monoxide protects hepatocytes from TNF-alpha/actinomycin D by inhibition of the caspase-8-mediated apoptotic pathway. Biochem Biophys Res Commun. 2006; 344:1172–1178. [PubMed: 16647044]
35. Sass G, Seyfried S, Parreira Soares M, Yamashita K, Kaczmarek E, Neuhuber WL, Tiegs G. Cooperative effect of biliverdin and carbon monoxide on survival of mice in immune-mediated liver injury. Hepatology. 2004; 40:1128–1135. [PubMed: 15486963]
36. Wen T, Zhao JY, Mei S, Guan L, Zhang YL. Protective effect of heme oxygenase-1 and its reaction product, carbon monoxide on acute liver injury induced by carbon tetrachloride in rats. Beijing Da Xue Xue Bao. 2006; 38:618–622. [PubMed: 17173083]
37. Sass G, Soares MC, Yamashita K, Seyfried S, Zimmermann WH, Eschenhagen T, Kaczmarek E, Ritter T, Volk HD, Tiegs G. Heme oxygenase-1 and its reaction product, carbon monoxide, prevent inflammation-related apoptotic liver damage in mice. Hepatology. 2003; 38:909–918. [PubMed: 14512878]
38. Ke B, Buelow R, Shen XD, Melinek J, Amersi F, Gao F, Ritter T, Volk HD, Busuttil RW, Kupiec-Weglinski JW. Heme oxygenase 1 gene transfer prevents CD95/Fas ligand-mediated apoptosis and improves liver allograft survival via carbon monoxide signaling pathway. Hum Gene Ther. 2002; 13:1189–1199. [PubMed: 12133272]

39. Kato GJ, Martyr S, Blackwelder WC, Nichols JS, Coles WA, Hunter LA, Brennan ML, Hazen SL, Gladwin MT. Levels of soluble endothelium-derived adhesion molecules in patients with sickle cell disease are associated with pulmonary hypertension, organ dysfunction, and mortality. Br J Haematol. 2005; 130:943–953. [PubMed: 16156864]
40. Beutler E. The effect of carbon monoxide on red cell life span in sickle cell disease. Blood. 1975; 46:253–259. [PubMed: 237591]
41. Huy NT, Xuan Trang DT, Uyen DT, Sasai M, Harada S, Kamei K. An improved colorimetric method for quantitation of heme using tetramethylbenzidine as substrate. Anal Biochem. 2005; 344:289–291. [PubMed: 16091279]
42. Dupuy AJ, Fritz S, Largaespada DA. Transposition and gene disruption in the male germline of the mouse. Genesis. 2001; 30:82–88. [PubMed: 11416868]
43. Vigdal TJ, Kaufman CD, Izsvak Z, Voytas DF, Ivics Z. Common physical properties of DNA affecting target site selection of sleeping beauty and other Tc1/mariner transposable elements. J Mol Biol. 2002; 323:441–452. [PubMed: 12381300]
44. Clark KJ, Geurts AM, Bell JB, Hackett PB. Transposon vectors for gene-trap insertional mutagenesis in vertebrates. Genesis. 2004; 39:225–233. [PubMed: 15286994]
45. Carlson CM, Dupuy AJ, Fritz S, Roberg-Perez KJ, Fletcher CF, Largaespada DA. Transposon mutagenesis of the mouse germline. Genetics. 2003; 165:243–256. [PubMed: 14504232]
46. Kren BT, Ghosh SS, Linehan CL, Roy-Chowdhury N, Hackett PB, Roy-Chowdhury J, Steer CJ. Hepatocyte-targeted delivery of Sleeping Beauty mediates efficient gene transfer in vivo. Gene Ther Mol Biol. 2003; 7:229–238.
47. Batzlsperger CA, Achatz S, Spreng J, Riegger GA, Griese DP. Evidence for a possible inhibitory interaction between the HO-1/CO- and Akt/NO-pathways in human endothelial cells. Cardiovasc Drugs Ther. 2007; 21:347–355. [PubMed: 17896171]
48. Lin Q, Weis S, Yang G, Weng YH, Helston R, Rish K, Smith A, Bordner J, Polte T, Gaunitz F, Dennery PA. Heme oxygenase-1 protein localizes to the nucleus and activates transcription factors important in oxidative stress. J Biol Chem. 2007; 282:20621–20633. [PubMed: 17430897]
49. Hori R, Kashiba M, Toma T, Yachie A, Goda N, Makino N, Soejima A, Nagasawa T, Nakabayashi K, Suematsu M. Gene transfection of H25A mutant heme oxygenase-1 protects cells against hydroperoxide-induced cytotoxicity. J Biol Chem. 2002; 277:10712–10718. [PubMed: 11786534]

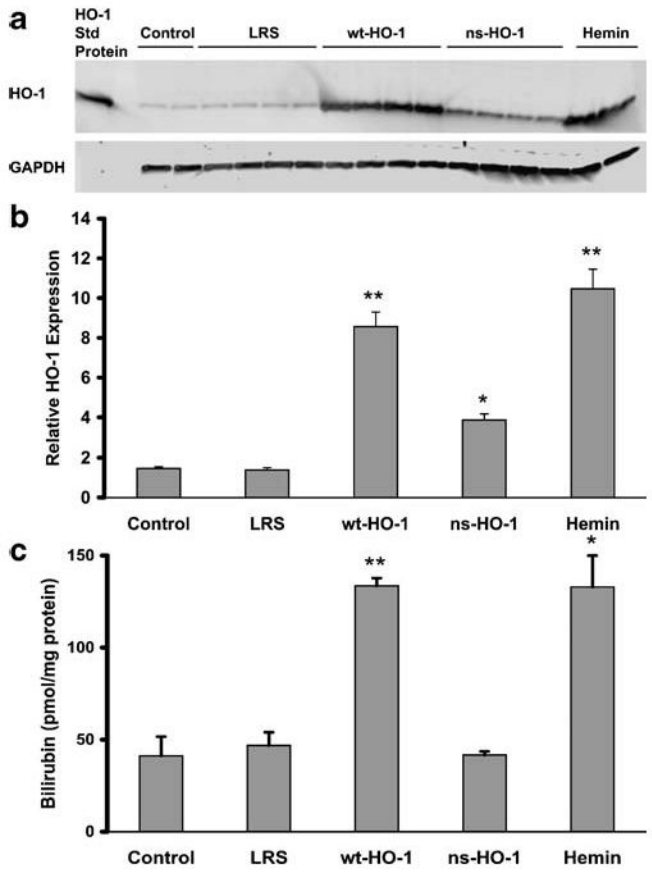

Fig. 1.

After 8 weeks, HO-1 protein expression is increased in the livers of sickle mice injected with *SB*-wt-HO-1, *SB*-ns-HO-1, or hemin. S+S-Antilles sickle mice were injected hydrodynamically with an albumin promoter-driven *SB* transposase vector with either a wild-type rat *hmox-1* gene (*wt-HO-1*) or a nonsense rat *hmox-1* gene (*ns-HO-1*) containing an early stop codon. Control sickle mice were either not injected (*control*), injected hydrodynamically with lactated Ringer's solution (*LRS*), or injected three consecutive days with hemin (*hemin*). Seven to 8 weeks after hydrodynamic injection or 18 h after the third hemin injection, the livers were removed and flash frozen. Microsomal membranes (n=2–4 mice per treatment group) were isolated from the livers, and 30 μg of microsomal protein from each liver was run on a western blot and immunostained for HO-1 and GAPDH protein expression (**a**). HO-1 protein bands at 32 kDa were quantified by densitometry (**b**). HO enzyme activity is increased in the livers of sickle mice injected with *SB*-wt-HO-1 or hemin, but not in control, LRS- or *SB*-ns-HO-1-treated mice (**c**). HO enzymatic activity was measured using 2 mg of liver microsomes per reaction (n=4 mice per treatment group) by measuring bilirubin production. Values are means±SEM, *p<0.05 and **p<0.01 compared to LRS controls using one-way ANOVA

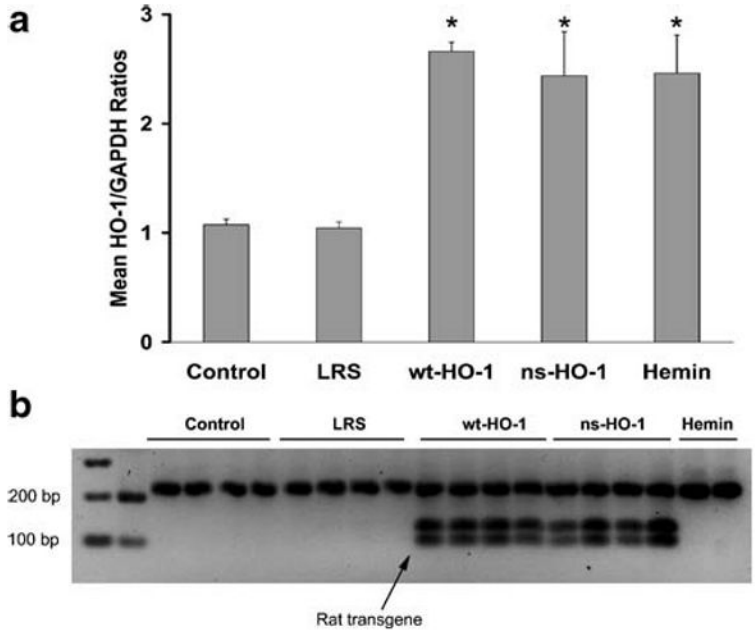

Fig. 2.

After 8 weeks, rat *hmox-1* mRNA is present in mouse livers. *Hmox*-1 mRNA was measured by qRT-PCR using total RNA isolated from livers. HO-1 to GAPDH mRNA ratios were higher in the livers of sickle mice injected with *SB*-wt-HO-1, *SB*-ns-HO-1, or hemin compared to LRS controls (**a**). Values are mean±SEM, **p*<0.05 compared to LRS controls using one-way ANOVA. Rat and mouse *hmox-1* RT-PCR products from mouse livers were differentiated by RFLP analysis using *ApaI* restriction enzyme digestion. The rat *hmox-1* sequence has an *ApaI* restriction site, and the mouse *hmox-1* sequence does not. The mouse fragment is 212 bp, and the rat fragments are 92 and 120 bp. Rat *hmox-1* mRNA was present in the livers of sickle mice injected with *SB*-wt-HO-1 or *SB*-ns-HO-1, but not in control, LRS-, or hemin-treated mice (**b**). Endogenous mouse *hmox-1* mRNA was present in all mouse livers

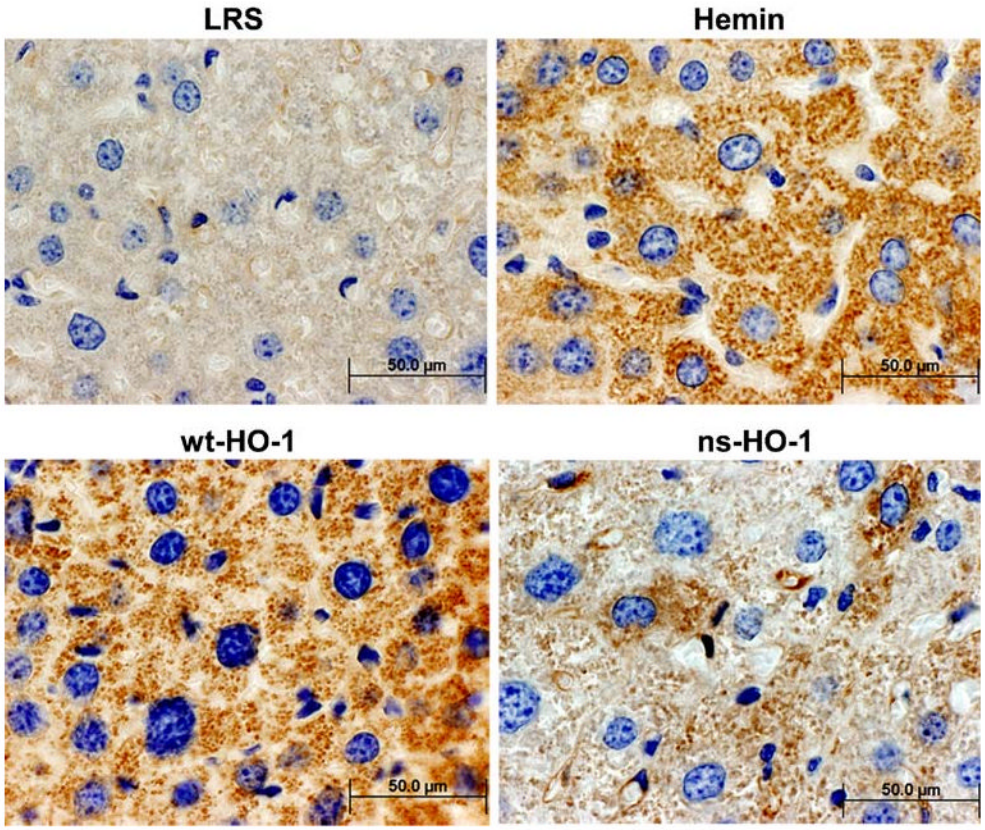

Fig. 3.

Immunohistochemistry demonstrates HO-1 overexpression in hepatocytes. Formalin-fixed paraffin embedded liver tissues were sectioned and stained with anti-HO-1. Sites of primary antibody binding were visualized with HRP-conjugated secondary IgG. HO-1/HRP immunoconjugates were detected with diaminobenzidine and H_2O_2. Nuclei were counter-stained with hematoxylin

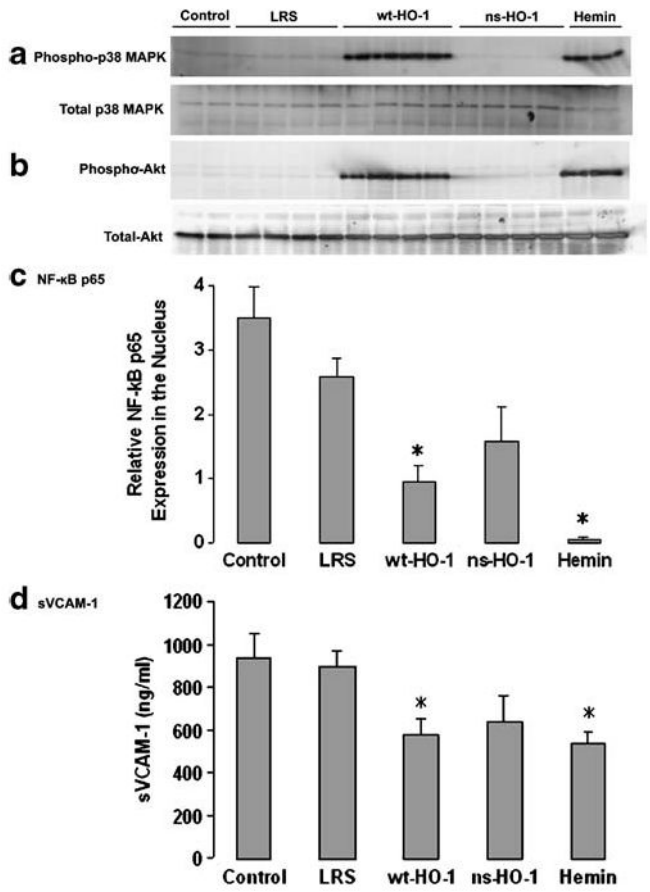

Fig. 4.

After 8 weeks, cytoprotective pathways are activated in sickle mice overexpressing wt-HO-1. Nuclear phospho-p38 MAPK (**a**) and phospho-Akt (**b**) were increased in mice injected with *SB*-wt-HO-1 or hemin, but not in control, LRS-, or *SB*-ns-HO-1-treated mice. Total nuclear p38 MAPK (**a**) and Akt (**b**) were not different between treatment groups. NF-κB p65 was decreased in liver nuclear extracts of sickle mice injected with *SB*-wt-HO-1 or hemin, but not in control, LRS-, or *SB*-ns-HO-1-treated mice (**c**). sVCAM-1 was lower in serum from sickle mice injected with *SB*-wt-HO-1 ($p<0.05$) or hemin ($p< 0.05$), but not in control or *SB*-ns-HO-1-treated mice compared to LRS mice (**d**). Nuclear extracts were isolated from livers, and 30 μg of nuclear extract protein from each liver was run on a western blot and immunostained for phospho- and total p38 (**a**) and Akt (**b**), and NF-κB p65. NF-κB p65 protein bands at 65 kDa were quantified by densitometry (**c**). Serum levels of sVCAM-1 were measured by ELISA (**d**). Values are mean±SEM; n=2–4 mice per treatment group; *$p<0.05$ compared to LRS controls using one-way ANOVA

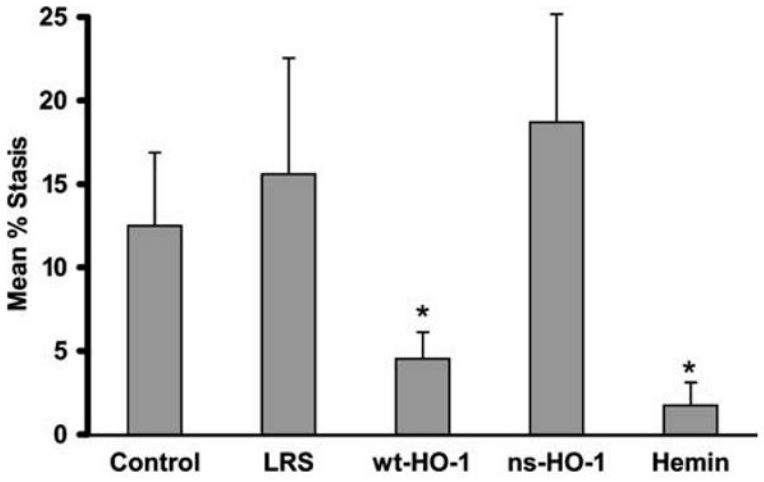

Fig. 5.

After 8 weeks, hypoxia-induced vascular stasis is inhibited in the skin of sickle mice injected with *SB*-wt-HO-1 or hemin, but not in control, LRS-, or *SB*-ns-HO-1-treated mice. Vascular stasis was measured in a DSFC model after hypoxia–reoxygenation. At baseline in room air, the mice were placed under a microscope, and flowing venules were selected inside the DSFC. The mice were then subjected to 1 h of hypoxia (7% O_2/93% N_2) followed by 1 h of reoxygenation in room air. After 1 h of reoxygenation, the same venules were re-examined for blood flow. The number of static venules exhibiting no blood flow were counted and expressed as a percentage of the total number of venules examined. There were seven mice and 403 venules in the control group, five mice and 243 venules in the LRS group, five mice and 347 venules in the wt-HO-1 group, six mice and 325 venules in the ns-HO-1 group, and five mice and 227 venules in the hemin group. There was a minimum of 26 venules per mouse. Values are mean %stasis±SEM. The proportions of venules exhibiting stasis in each treatment group were compared using a *Z* test; *$p<0.05$ compared to LRS controls

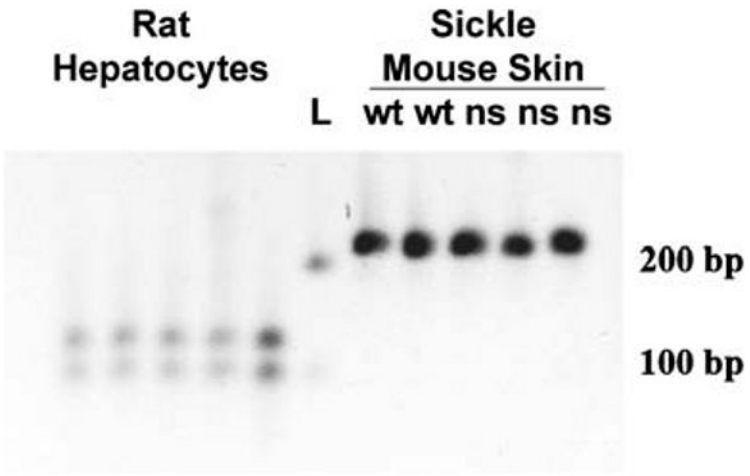

Fig. 6.

Rat HO-1 mRNA is not expressed in dorsal skin. The dorsal skin of sickle mice was examined for the presence of rat *hmox-1* mRNA by qRT-PCR RFLP analysis. The rat *hmox-1 ApaI* fragments at 92 and 120 bp were absent in the dorsal skin samples. The mouse product at 212 bp was seen in the skin of all mice. Rat hepatocytes were analyzed by qRT-PCR RFLP as controls and show the rat *hmox-1* fragments at 92 and 120 bp but not the mouse product at 212 bp. The lane marked *L* designates DNA ladder